

Deautoconvolution in the two-dimensional case

YU DENG*, BERND HOFMANN† and FRANK WERNER‡

October 26, 2022

Abstract: There is extensive mathematical literature on the inverse problem of deautoconvolution for a function with support in the unit interval $[0, 1] \subset \mathbb{R}$, but little is known about the multidimensional situation. This article tries to fill this gap with analytical and numerical studies on the reconstruction of a real function of two real variables over the unit square from observations of its autoconvolution on $[0, 2]^2 \subset \mathbb{R}^2$ (full data case) or on $[0, 1]^2$ (limited data case). In an L^2 -setting, twofoldness and uniqueness assertions are proven for the deautoconvolution problem in 2D. Moreover, its ill-posedness is characterized and illustrated. Extensive numerical case studies give an overview of the behaviour of stable approximate solutions to the two-dimensional deautoconvolution problem obtained by Tikhonov-type regularization with different penalties and the iteratively regularized Gauss-Newton method.

Keywords: deautoconvolution, inverse problem, ill-posedness, case studies in 2D, Tikhonov-type regularization, iteratively regularized Gauss-Newton method

AMS-classification (2010): 47J06, 65R32, 45Q05, 47A52, 65J20

1 Introduction

The object of research in this work is the problem of *deautoconvolution*, where our focus is on the *two-dimensional case*, which means that a square integrable real function of two variables $x(t_1, t_2)$ ($0 \leq t_1, t_2 \leq 1$) is to be identified from the function $y = x * x$ of its autoconvolution. If we consider x as an element in the Hilbert space $L^2(\mathbb{R}^2)$ with support $\text{supp}(x) \subseteq [0, 1]^2$, then it is well-known that $x * x$ also lies in $L^2(\mathbb{R}^2)$ with support $\text{supp}(x * x) \subseteq [0, 2]^2$. In this context, the elements x and $x * x$ both can be considered as tempered distributions with compact support, where $\text{supp}(\cdot)$ is regarded as the essential support with respect to the Lebesgue measure λ in \mathbb{R}^2 . Instead of y itself, noisy data $y^\delta \in L^2(\mathbb{R}^2)$ to y with some noise level $\delta \geq 0$ are available only. Since the inverse problem of deautoconvolution tends to be ill-posed, the aim of the recovery process is to find *stable approximate solutions* of x based on the data y^δ . We are going to distinguish the *full data case*, where noisy data are available for $y(s_1, s_2)$ ($0 \leq s_1, s_2 \leq 2$), and the *limited data case*, where data are given for $y(s_1, s_2)$ ($0 \leq s_1, s_2 \leq 1$). Since the scope of the data in the limited data case is only 25% compared to the full data case, the effect of ill-posedness is stronger in that

*Chemnitz University of Technology, Faculty of Mathematics, 09107 Chemnitz, Germany, e-mail: yu.deng@math.tu-chemnitz.de

†Faculty of Mathematics, Chemnitz University of Technology, 09107 Chemnitz, Germany, e-mail: hofmannb@mathematik.tu-chemnitz.de.

‡Institute for Mathematics, University of Würzburg, Emil-Fischer-Str. 30, 97074 Würzburg, Germany, e-mail: frank.werner@mathematik.uni-wuerzburg.de

case. As a consequence, also the chances for the accurate recovery of x are more restricted in the limited data case.

The simplest application of our deautoconvolution problem in two dimensions is the recovery of the density function x with support in the unit square $[0, 1]^2$ of a two-dimensional random variable \mathfrak{X} from observations of the density function y of the two-dimensional random variable $\mathfrak{Y} := \hat{\mathfrak{X}} + \bar{\mathfrak{X}}$, where \mathfrak{X} , $\hat{\mathfrak{X}}$ and $\bar{\mathfrak{X}}$ are assumed to be of i.i.d. type.

The deautoconvolution problem *in one dimension* has been considered extensively in the literature motivated by physical applications in spectroscopy (see, e.g., [6, 29]). Its mathematical analysis has been implemented comprehensively in the last decades with focus on properties of the specific forward operator, ill-posedness and regularization based on the seminal paper [20]. In this context, we refer to [8, 10, 11, 14, 16, 17, 23] for investigations concerning the stable identification of real functions x on the unit interval $[0, 1]$ from noisy data of its autoconvolution $x * x$. A new series of interdisciplinary autoconvolution studies was unleashed by a cooperation started in 2010 between a Research Group of the Max Born Institute for Nonlinear Optics and Short Pulse Spectroscopy, Berlin, led by Prof. Günter Steinmeyer and the Chemnitz research Group on Regularization, and we refer to the publications [3, 9, 18, 19] presenting the output of this cooperation. The goal of this cooperation between mathematics and laser optics was the extension of the one-dimensional deautoconvolution problem to complex-valued functions combining amplitude and phase functions for characterizing ultrashort laser pulses.

In this article, in an L^2 -setting we are considering a series of numerical case studies for the *nonlinear Volterra-type integral equation*

$$F(x) = y, \quad \text{with } F(x) := x * x, \quad (1)$$

the solution of which solves the *deautoconvolution problem in two dimensions*. Equation (1) is a special case of a nonlinear operator equation

$$F(x) = y, \quad F : \mathcal{D}(F) \subseteq X \rightarrow Y, \quad (2)$$

with *forward operator* F mapping between *real-valued Hilbert spaces* X and Y with norms $\|\cdot\|_X$ and $\|\cdot\|_Y$, respectively, and domain $\mathcal{D}(F)$.

In dependence of the data situation, we have to distinguish in the full data case the forward operator $F : X = L^2([0, 1]^2) \rightarrow Y = L^2([0, 2]^2)$ defined as

$$[F(x)](s_1, s_2) := \int_{\max(s_2-1, 0)}^{\min(s_2, 1)} \int_{\max(s_1-1, 0)}^{\min(s_1, 1)} x(s_1 - t_1, s_2 - t_2) x(t_1, t_2) dt_1 dt_2 \quad (0 \leq s_1, s_2 \leq 2) \quad (3)$$

and in the limited data case the forward operator $F : X = L^2([0, 1]^2) \rightarrow Y = L^2([0, 1]^2)$ as

$$[F(x)](s_1, s_2) := \int_0^{s_2} \int_0^{s_1} x(s_1 - t_1, s_2 - t_2) x(t_1, t_2) dt_1 dt_2 \quad (0 \leq s_1, s_2 \leq 1). \quad (4)$$

In general we consider $\mathcal{D}(F) = X = L^2([0, 1]^2)$, but for the limited data case we partially focus on *non-negative solutions* expressed by the domain $\mathcal{D}(F) = \mathcal{D}^+$ with

$$\mathcal{D}^+ := \{x \in X = L^2([0, 1]^2) : x \geq 0 \text{ a.e. on } [0, 1]^2\}. \quad (5)$$

For any function $x \in L^2([0, 1]^2)$ the autoconvolution products $F(x) = x * x$ and $F(-x) = (-x) * (-x)$ coincide for both forward operator versions (3) and (4). However, it is of interest whether for $y = x * x$ the elements x and $-x$ are the only solutions of equation (1) or not. Moreover it is of interest whether in the limited data case the restriction of the domain $\mathcal{D}(F)$ to \mathcal{D}^+ from (5) leads to unique solutions. Some answers to those questions will be given in the subsequent Section 2.

The remainder of the paper is organized as follows: Section 2 is devoted to assertions on twofoldness and uniqueness for the deautoconvolution problem in two dimensions, preceded by a subsection

with relevant lemmas and definitions. As an inverse problem, deautoconvolution tends to be ill-posed in the setting of infinite dimensional L^2 -spaces. After the presentation of two functions defined over the unit square as basis for later numerical case studies, in Section 3 the specific ill-posedness character for the deautoconvolution of a real function of two real variables with compact support is analyzed and illustrated. To suppress ill-posedness phenomena, variants of variational and iterative regularization methods are used, which will be introduced in Section 4. The numerical treatment, including discretization approaches of forward operator and penalty functionals for the Tikhonov regularization as well as for the iterative regularization by using the Fourier transform, is outlined in Section 5. Section 6 completes the article with comprehensive numerical case studies.

2 Assertions on twofoldness and uniqueness for the deautoconvolution problem in two dimensions

2.1 Preliminaries

Assertions on twofoldness and uniqueness for the deautoconvolution problem in one dimension have been formulated in the articles [20] for the limited data case and [19] for the full data case. The respective proofs are based on the Titchmarsh convolution theorem from [31], which was formulated as Lemma 3 in [20] and will be recalled below in a slightly reformulated form as Lemma 1.

Lemma 1. *Let the functions $f, g \in L^2(\mathbb{R})$ have compact supports $\text{supp}(f)$ and $\text{supp}(g)$. Then we have for the convolution that $f * g \in L^2(\mathbb{R})$ and that the equation*

$$\inf \text{supp}(f * g) = \inf \text{supp}(f) + \inf \text{supp}(g) \quad (6)$$

holds. In particular, for $\text{supp}(f)$ and $\text{supp}(g)$ covered by the unit interval $[0, 1]$, we conclude from

$$[f * g](s) = \int_{\max(s-1, 0)}^{\min(s, 1)} f(s-t) g(t) dt = 0 \quad \text{a.e. for } s \in [0, \gamma] \quad (\gamma \leq 2)$$

that there are numbers $\gamma_1, \gamma_2 \in [0, 1]$ with $\gamma_1 + \gamma_2 \geq \gamma$ such that

$$f(t) = 0 \quad \text{a.e. for } t \in [0, \gamma_1] \quad \text{and} \quad g(t) = 0 \quad \text{a.e. for } t \in [0, \gamma_2].$$

For an extension of the Titchmarsh convolution theorem to two dimensions, we mention the following Lemma 2 (cf. [26, 27]).

Lemma 2. *Let the functions $f, g \in L^2(\mathbb{R}^2)$ have compact supports $\text{supp}(f)$ and $\text{supp}(g)$. Then we have for the convolution that $f * g \in L^2(\mathbb{R}^2)$ and that the equation*

$$\text{ch } \text{supp}(f * g) = \text{ch } \text{supp}(f) + \text{ch } \text{supp}(g) \quad (7)$$

*holds, where $\text{ch } M$ denotes the convex hull of a set $M \subseteq \mathbb{R}^2$. In the special case that $\text{supp}(f * g) = \emptyset$ we have that at least one of the supports $\text{supp}(f)$ or $\text{supp}(g)$ is the empty set.*

Definition 1. *For given $y \in L^2([0, 2]^2)$, we call $x^\dagger \in L^2([0, 1]^2)$ with $\text{supp}(x^\dagger) \subseteq [0, 1]^2$ a solution to the operator equation (1) in the full data case if it satisfies the condition*

$$[x^\dagger * x^\dagger](s_1, s_2) = y(s_1, s_2) \quad \text{a.e. for } (s_1, s_2) \in [0, 2]^2. \quad (8)$$

Definition 2. *For given $y \in L^2([0, 1]^2)$, we call $x^\dagger \in L^2([0, 1]^2)$ with $\text{supp}(x^\dagger) \subseteq [0, 1]^2$ a solution to the operator equation (1) in the limited data case if it satisfies the condition*

$$[x^\dagger * x^\dagger](s_1, s_2) = y(s_1, s_2) \quad \text{a.e. for } (s_1, s_2) \in [0, 1]^2. \quad (9)$$

For $x^\dagger \in \mathcal{D}^+$ with \mathcal{D}^+ from (5) we call it non-negative solution in the limited data case.

Definition 3. We call $x \in L^2([0, 1]^2)$ with $\text{supp}(x) \subseteq [0, 1]^2$ satisfying (8) or (9) a factored solution to equation (1) in the full data case or in the limited data case, respectively, if we have the structure $x(t_1, t_2) = x_1(t_1)x_2(t_2)$ ($0 \leq t_1, t_2 \leq 1$) with $x_i \in L^2([0, 1])$, $\text{supp}(x_i) \subseteq [0, 1]$ for $i = 1$ and $i = 2$. If moreover $x_i \geq 0$ a.e. on $[0, 1]$ for $i = 1$ and $i = 2$, then we call it non-negative factored solution in the respective case.

2.2 Results for the full data case

Lemma 2 allows us to prove the following theorem for the forward autoconvolution operator $F : L^2([0, 1]^2) \rightarrow L^2([0, 2]^2)$ from (3), which is an extension of [19, Theorem 4.2] to the two-dimensional case of the deautoconvolution problem.

Theorem 1. *If, for given $y \in L^2([0, 2]^2)$, the function $x^\dagger \in L^2([0, 1]^2)$ with $\text{supp}(x^\dagger) \subseteq [0, 1]^2$ is a solution to (1) with F from (3), then x^\dagger and $-x^\dagger$ are the only solutions of this equation in the full data case.*

Proof. Let $x^\dagger \in L^2([0, 1]^2)$ supposing $\text{supp}(x^\dagger) \subseteq [0, 1]^2$ and $h \in L^2([0, 1]^2)$ supposing $\text{supp}(h) \subseteq [0, 1]^2$. We assume that x^\dagger and $x^\dagger + h$ solve the equation (1), which means that $[x^\dagger * x^\dagger](s_1, s_2) = [(x^\dagger + h) * (x^\dagger + h)](s_1, s_2)$ a.e. for $(s_1, s_2) \in [0, 2]^2$. Then we have $[(x^\dagger + h) * (x^\dagger + h) - x^\dagger * x^\dagger](s_1, s_2) = [h * (2x^\dagger + h)](s_1, s_2) = 0$ a.e. for $(s_1, s_2) \in [0, 2]^2$. By setting $f := h$ and $g := 2x^\dagger + h$ we now apply Lemma 2. Taking into account that $\text{supp}(h * (2x^\dagger + h)) \subseteq [0, 2]^2$ we then have $\text{supp}(h * (2x^\dagger + h)) = \emptyset$ and consequently also $\text{ch supp}(h * (2x^\dagger + h)) = \emptyset$. This implies due to equation (7) that either $\text{supp}(h) = \emptyset$ or $\text{supp}(2x^\dagger + h) = \emptyset$. On the one hand, $\text{supp}(h) = \emptyset$ leads to the solution x^\dagger itself, whereas on the other hand $\text{supp}(2x^\dagger + h) = \emptyset$ leads to $[2x^\dagger + h](t_1, t_2) = 0$ a.e. for $(t_1, t_2) \in [0, 1]^2$ and consequently with $h = -2x^\dagger$ to the second solution $-x^\dagger$. Alternative solutions are thus excluded, which proves the theorem. \square

2.3 Results for the limited data case

For solutions $x^\dagger \in L^2([0, 1]^2)$ to equation (1) with $\text{supp}(x^\dagger) \subseteq [0, 1]^2$, the condition $0 \in \text{supp}(x^\dagger)$ plays a prominent role in the limited data case. This condition means that for any ball $B_r(0)$ around the origin with arbitrary small radius $r > 0$ there exists a set $M_r \subset B_r(0) \cap [0, 1]^2$ with Lebesgue measure $\lambda(M_r) > 0$ such that $x^\dagger(t_1, t_2) \neq 0$ a.e. for $(t_1, t_2) \in M_r$. Vice versa, for $0 \notin \text{supp}(x^\dagger)$ we have some sufficiently small radius $r > 0$ such that $x^\dagger(t_1, t_2) = 0$ a.e. for $(t_1, t_2) \in B_r(0) \cap [0, 1]^2$.

First, we generalize in Theorem 2 those aspects of [20, Theorem 1] that concern the strong non-injectivity of the autoconvolution operator in the limited data case.

Theorem 2. *If, for given $y \in L^2([0, 1]^2)$, the function $x^\dagger \in L^2([0, 1]^2)$ with $\text{supp}(x^\dagger) \subseteq [0, 1]^2$ is a solution to (1) with F from (4) that fulfils the condition*

$$0 \notin \text{supp}(x^\dagger), \quad (10)$$

then there exist infinitely many other solutions $\hat{x}^\dagger \in L^2([0, 1]^2)$ to (1) with $\text{supp}(\hat{x}^\dagger) \subseteq [0, 1]^2$ in the limited data case.

Proof. If (10) holds, there is some $0 < \varepsilon < 1/2$ such that $x^\dagger(t_1, t_2) = 0$ a.e. for $(t_1, t_2) \in [0, \varepsilon]^2$. Then we have, for all elements $h \in L^2([0, 1]^2)$ with $\text{supp}(h) \subseteq [0, 1]^2$ satisfying the condition

$$h(t_1, t_2) = 0 \quad \text{a.e. for } (t_1, t_2) \in [0, 1]^2 \setminus [1 - \varepsilon, 1]^2,$$

that $\hat{x}^\dagger = x^\dagger + h$ obeys the condition

$$[\hat{x}^\dagger * \hat{x}^\dagger](s_1, s_2) = y(s_1, s_2) \quad \text{a.e. for } (s_1, s_2) \in [0, 1]^2.$$

This is a consequence of the fact that $[h * (2x^\dagger + h)](s_1, s_2) = 0$ a.e. for $(s_1, s_2) \in [0, 1]^2$ is true for each such element h . \square

To formulate uniqueness assertions for solutions x^\dagger to equation (1) in the limited data case, we restrict our considerations now to non-negative solutions and the domain $\mathcal{D}(F) = \mathcal{D}^+$ from (5) for the forward operator F from (4). We present in Theorem 3 a result that extends to the two-dimensional autoconvolution operator $F : \mathcal{D}^+ \subset L^2([0, 1]^2) \rightarrow L^2([0, 1]^2)$ from (4) those aspects of [20, Theorem 1] which concern the solution uniqueness. Precisely, we are able to handle the special case of *factored non-negative solutions* in the sense of Definition 3, occurring for example when x^\dagger is a density function for the two-dimensional random variable $\mathfrak{X} = (\mathfrak{X}_1, \mathfrak{X}_2)$, where \mathfrak{X}_1 and \mathfrak{X}_2 are uncorrelated one-dimensional random variables.

Theorem 3. *Let, for given $y \in L^2([0, 1]^2)$, x^\dagger be a non-negative factored solution to equation (1) in the limited data case, which satisfies the condition*

$$0 \in \text{supp}(x^\dagger). \quad (11)$$

Then there are no other non-negative factored solutions in this case.

Proof. For the factored situation, we have that the right-hand side y is also factored with

$$y(s_1, s_2) = y_1(s_1) y_2(s_2) \quad (0 \leq s_1, s_2 \leq 1) \quad \text{and} \quad y_1 = x_1^\dagger * x_1^\dagger, \quad y_2 = x_2^\dagger * x_2^\dagger.$$

Moreover, the condition (11) implies that

$$\inf \text{supp}(x_1^\dagger) = \inf \text{supp}(x_2^\dagger) = 0. \quad (12)$$

Otherwise, there would be a square $[0, \varepsilon]^2$ with $\varepsilon = \max\{\inf \text{supp}(x_1^\dagger), \inf \text{supp}(x_2^\dagger)\} > 0$ on which x^\dagger vanishes almost everywhere such that $0 \notin \text{supp}(x^\dagger)$ would then apply. Now we suppose that for $i = 1$ and $i = 2$ quadratically integrable perturbations $h_i(t_i)$ ($0 \leq t_i \leq 1$) exist such that $x_i^\dagger + h_i \geq 0$ a.e. on $[0, 1]$ and

$$(x_1^\dagger + h_1) * (x_1^\dagger + h_1) = y_1 \quad \text{and} \quad (x_2^\dagger + h_2) * (x_2^\dagger + h_2) = y_2. \quad (13)$$

To complete the proof of the theorem we still show that h_1 and h_2 have to vanish almost everywhere on $[0, 1]$. This can be done with the help of Titchmarsh's convolution theorem in the one-dimensional case (cf. Lemma 1). From (13) we derive for $i = 1$ and $i = 2$ that

$$[h_i * (2x_i^\dagger + h_i)](s_i) = 0 \quad \text{a.e. for } s_i \in [0, 1],$$

where $x_i^\dagger + h_i \geq 0$ implies that $2x_i^\dagger + h_i \geq x_i^\dagger$ and $\inf \text{supp}(2x_i^\dagger + h_i) = 0$ as a consequence of (12). Then it follows from Lemma 1 that

$$\inf \text{supp}(h_i) + \inf \text{supp}(2x_i^\dagger + h_i) = \inf \text{supp}(h_i * (2x_i^\dagger + h_i)) \geq 1$$

and hence $\inf \text{supp}(h_i) \geq 1$ for both $i = 1, 2$, which gives $h_i = 0$ a.e. on $[0, 1]$ and completes the proof. \square

3 Examples and ill-posedness phenomena of deautoconvolution in 2D

3.1 Two Examples

For the numerical case studies of deautoconvolution in 2D, we have selected two examples of solutions x^\dagger to the autoconvolution equation in 2D. The first example refers to the function

$$x^\dagger(t_1, t_2) = \left(-3t_1^2 + 3t_1 + \frac{1}{4}\right) (\sin(1.5\pi t_2) + 1) \quad (0 \leq t_1, t_2 \leq 1) \quad (14)$$

to be reconstructed from its own autoconvolution $F(x^\dagger) = x^\dagger * x^\dagger$. This *smooth and non-negative factored* function x^\dagger is illustrated in Figure 1, in a line with the $F(x^\dagger)$ -images for the limited and full data case, respectively.

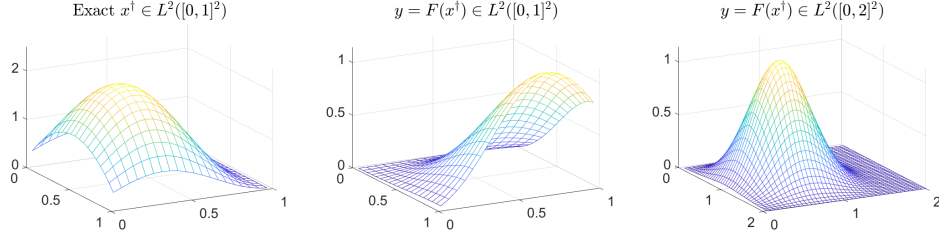


Figure 1: Smooth factored function $x^\dagger(t_1, t_2)$ and $F(x^\dagger)$ with limited data and full data, respectively.

The second example refers to the *non-smooth, non-factored* and non-negative solution

$$x^\dagger(t_1, t_2) = \begin{cases} \sin(1.5\pi(t_1 + t_2)) + 1 & (0 \leq t_1 \leq 0.5, 0 \leq t_2 \leq 1) \\ 1 & (0.5 < t_1 \leq 1, 0 \leq t_2 \leq 1) \end{cases}, \quad (15)$$

which is illustrated in Figure 2, again in a line with $F(x^\dagger)$ -images for the limited and full data case, respectively.

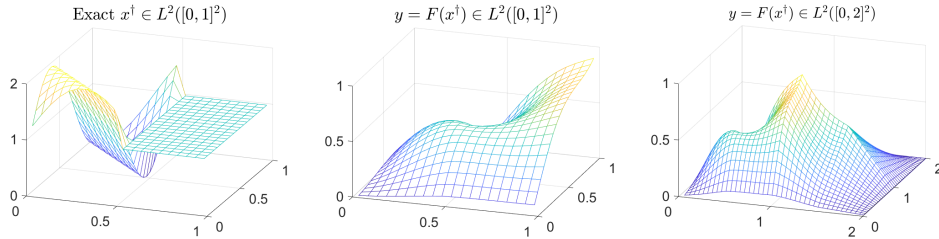


Figure 2: Non-smooth non-factored function $x^\dagger(t_1, t_2)$ and $F(x^\dagger)$ with limited data and full data, respectively.

3.2 Ill-posedness phenomenon

As we will see in particular for the case of limited data in the numerical case studies to be presented below, least-squares solutions to the discretized two-dimensional problem of deautoconvolution tend to become strongly oscillating even if the noise level $\delta > 0$ in the observed right-hand side y^δ is small. This indicates instability as a phenomenon of *ill-conditioning* for a discretized variant of deautoconvolution and of *ill-posedness* for the underlying operator equation (1) in infinite dimensional L^2 -spaces. For a theoretical verification we adopt the *concept of local ill-posedness* along the lines of [21, Def. 1.1] for nonlinear operator equations, and we recall this concept by the following definition.

Definition 4. An operator equation $F(x) = y$ with nonlinear forward operator $F : \mathcal{D}(F) \subseteq X \rightarrow Y$ mapping between the Hilbert spaces X and Y with domain $\mathcal{D}(F)$ is called *locally ill-posed at a solution point* $x^\dagger \in \mathcal{D}(F)$ if there exist for all closed balls $\overline{\mathcal{B}}_r(x^\dagger)$ with radius $r > 0$ and center x^\dagger sequences $\{x_n\} \subset \overline{\mathcal{B}}_r(x^\dagger) \cap \mathcal{D}(F)$ satisfying the condition

$$\|F(x_n) - F(x^\dagger)\|_Y \rightarrow 0, \quad \text{but} \quad \|x_n - x^\dagger\|_X \not\rightarrow 0, \quad \text{as} \quad n \rightarrow \infty.$$

Otherwise, the operator equation is called *locally well-posed at* x^\dagger .

Local ill-posedness everywhere on the non-negativity domain

$$\mathcal{D}(F) = \{x \in X = L^2([0, 1]) : x \geq 0 \text{ a.e. on } [0, 1]\}$$

was proven for the *one-dimensional* deautoconvolution problem in the limited data case in [20, Lemma 6]. With the following proposition we extend by using similar proof ideas this assertion to the two-dimensional case and $\mathcal{D}(F) = \mathcal{D}^+$ with \mathcal{D}^+ from (5). We should mention as an overall consequence of the observed ill-posedness that the *stable approximate solution* of the two-dimensional deautoconvolution problem *requires* the use of variational or iterative *regularization methods*.

Proposition 1. *For the limited data case, the operator equation (1) with $X = Y = L^2([0, 1]^2)$ and forward operator F from (4) restricted to the non-negativity domain $\mathcal{D}(F) = \mathcal{D}^+$ from (5) is locally ill-posed everywhere on \mathcal{D}^+ .*

Proof. Let $x^\dagger \in \mathcal{D}^+$ be a solution to the operator equation under consideration here. To show local ill-posedness at x^\dagger we introduce for fixed $r > 0$ a sequence $\{h_n\}_{n=3}^\infty$ of perturbations of the form

$$h_n(t_1, t_2) := \begin{cases} nr & \text{for } (t_1, t_2) \in [1 - \frac{1}{n}, 1]^2 \\ 0 & \text{for } (t_1, t_2) \in [0, 1]^2 \setminus [1 - \frac{1}{n}, 1]^2 \end{cases}$$

with $x_n := x^\dagger + h_n \in \mathcal{D}^+$, $\|h_n\|_{L^2([0, 1]^2)} = r$ and consequently $x_n \in \overline{\mathcal{B}_r(x^\dagger)} \cap \mathcal{D}^+$ for all $n \geq 3$. To complete the proof of the proposition we still need to show that the norm $\|F(x_n) - F(x^\dagger)\|_{L^2([0, 1]^2)}$ tends to zero as n tends to infinity. Due to the facts that $F(x_n) - F(x^\dagger) = 2x^\dagger * h_n + h_n * h_n$ and $\|h_n * h_n\|_{L^2([0, 1]^2)} = 0$, it is sufficient to show the limit condition

$$\|x^\dagger * h_n\|_{L^2([0, 1]^2)} \rightarrow 0 \quad \text{as } n \rightarrow \infty.$$

Evidently, the non-negative values

$$[x^\dagger * h_n](s_1, s_2) = \int_0^{s_2} \int_0^{s_1} h_n(s_1 - t_1, s_2 - t_2) x^\dagger(t_1, t_2) dt_1 dt_2$$

can be different from zero only for the pairs $(s_1, s_2) \in [1 - \frac{1}{n}, 1]^2$. Using the Cauchy-Schwarz inequality and taking into account that $x^\dagger \in \mathcal{D}^+$ we have for those pairs the estimate

$$[x^\dagger * h_n](s_1, s_2) = nr \int_0^{s_2 - (1 - \frac{1}{n})} \int_0^{s_1 - (1 - \frac{1}{n})} x^\dagger(t_1, t_2) dt_1 dt_2 \leq r \|x^\dagger\|_{L^2([0, 1]^2)}.$$

This, however, yields

$$\|x^\dagger * h_n\|_{L^2([0, 1]^2)} \leq r \|x^\dagger\|_{L^2([0, 1]^2)} \left(\int_{1 - \frac{1}{n}}^1 \int_{1 - \frac{1}{n}}^1 ds_1 ds_2 \right)^{1/2} = \frac{r \|x^\dagger\|_{L^2([0, 1]^2)}}{n}$$

tending to zero as n tends to infinity, which completes the proof. \square

In the full data case of one-dimensional deautoconvolution, local ill-posedness everywhere has been shown by Proposition 2.3 in [17]. The used counterexample, however, is much more sophisticated and requires perturbations with weak poles at the origin. This seems to indicate the significantly lower strength of ill-posedness for the full data case compared to the limited data case. For factored solutions, the counterexample from [17] can also be exploited to prove local ill-posedness for the two-dimensional deautoconvolution problem in the full data case. Numerical case studies confirm the lower level of instability in the full data case of the 2D deautoconvolution compared to the limited data case, and we refer to Figure 3 below.

Taking into account throughout the paper the *deterministic noise model*

$$\|y^\delta - y\|_Y \leq \delta, \tag{16}$$

we have calculated *discretized least-square solutions* x_{ls} of the deautoconvolution problem for the first example x^\dagger given in (14). In this context, a discretization with 21×21 grid points over the unit square has been exploited for minimizing the Euclidean norm squares of the discretized residuals $F(x^\dagger) - y^\delta$. By using a noise level $\delta > 0$ that corresponds to a relative data error of 0.8%, the least squares situations for $Y := L^2([0, 2]^2)$ of the full data case with F defined in (4) and for $Y := L^2([0, 1]^2)$ of the limited data case with F defined in (3) can be compared in Figure 3.

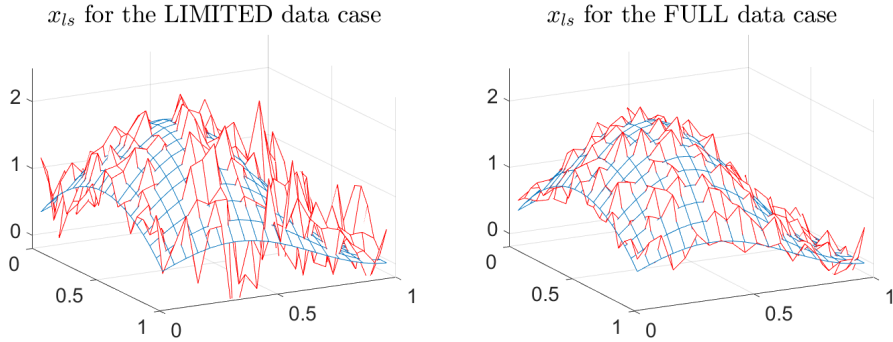


Figure 3: Phenomenon of ill-posedness of deautoconvolution.

As a consequence of the *ill-posedness phenomenon* of the deautoconvolution problem in 2D we see from the Figure 3 the occurrence of *strong oscillations* in both cases. The oscillations, however, are much heavier for the limited data case (left-hand graph) than for the full data case (right-hand graph). The difference is particularly pronounced for function values on the rear triangle half of the underlying unit square. The discretized L^2 -norms of the deviation $x_{ls} - x^\dagger$ correspond to relative errors of 34.54% (left) and 13.92% (right).

4 Regularization methods

4.1 Tikhonov regularization and regularization parameter choices

As a first approach to overcome the ill-posedness of the two-dimensional deautoconvolution problem, we adopt the variational (Tikhonov-type) regularization, which is well-developed for solving ill-posed nonlinear operator equations. For this approach, the stable approximate solutions (*regularized solutions*) x_α^δ are global minimizers of the optimization problem

$$T_\alpha^\delta(x) := \|F(x) - y^\delta\|_Y^2 + \alpha \mathcal{R}(x) \rightarrow \min_{x \in \mathcal{D}(F) \subseteq X}, \quad (17)$$

with *regularization parameter* $\alpha > 0$ and some *penalty functional* $\mathcal{R} : X \rightarrow [0, +\infty]$ possessing the domain $\mathcal{D}(\mathcal{R}) := \{x \in X = L^2([0, 1]^2) : \mathcal{R}(x) < \infty\}$. The penalty functional is assumed to be *stabilizing*, *convex* and *weakly sequentially continuous* such that for the autoconvolution operator F , which is *weakly sequentially closed*, the general theory of variational regularization (see, e.g. [30, Section 4.1] and [15, 28]) with respect to *existence*, *stability* and *convergence* of the Tikhonov-regularized solutions $x_\alpha^\delta \in \mathcal{D}(F) \cap \mathcal{D}(\mathcal{R})$ applies. The following three penalty functionals are under consideration in this study:

- Classical norm square penalty

$$\mathcal{R}_1(x) := \|x - \bar{x}\|_X^2,$$

with prescribed reference element $\bar{x} \in X$ and $\mathcal{D}(\mathcal{R}_1) = X$. Notably, $\bar{x} \in X$ expresses some a-priori knowledge about the potential solution.

- Gradient norm square penalty

$$\mathcal{R}_2(x) := \int_{[0,1]^2} \|\nabla x\|_2^2 dt_1 dt_2$$

where $\nabla x = (\frac{\partial x}{\partial t_1}, \frac{\partial x}{\partial t_2})$ denotes the gradient with respect to both variables t_1, t_2 and $\|\cdot\|_2$ is the Euclidean norm. Here, we have $\mathcal{D}(\mathcal{R}_2) = H^1([0, 1]^2)$. For this setting, the solution is assumed to have a certain smoothness.

- Total variation penalty

$$\mathcal{R}_3(x) := \|x\|_{TV([0,1]^2)} = \int_{[0,1]^2} \|\nabla x\|_1 dt_1 dt_2,$$

where $\mathcal{D}(\mathcal{R}_3) = BV([0, 1]^2) := \{x \in L^1([0, 1]^2) : \|x\|_{TV([0,1]^2)} < \infty\}$ is the space of bounded variation over the unit square $[0, 1]^2$. This approach is originally introduced for image restoration with the special aim of retaining the information on edges in an image, i.e., the penalty should work for solutions possessing jumps. A detailed analysis of TV-regularization can, for example, be found in [1, 12].

In a first step, we want to choose the optimal regularization parameter α_{opt} for each input noise level δ and corresponding y^δ according to

$$\alpha_{opt}(\delta) = \operatorname{argmin}_{\alpha > 0} \|x_\alpha^\delta - x^\dagger\|_X. \quad (18)$$

It is well-known that for the practical use of *a priori choices* for finding the regularization parameter $\alpha = \alpha(\delta)$, some smoothness information about the exact solution x^\dagger is required, which is normally not available. Therefore, *a posteriori choices* $\alpha = \alpha(\delta, y^\delta)$ are exploiting the measured noisy data y^δ in combination with knowledge of the noise level $\delta > 0$ are an appropriate alternative (cf. [15, Sect. 3.1]). Under the limit conditions

$$\alpha(\delta, y^\delta) \rightarrow 0 \quad \text{and} \quad \frac{\delta^2}{\alpha(\delta, y^\delta)} \rightarrow 0 \quad \text{as} \quad \delta \rightarrow 0 \quad (19)$$

the regularized solutions x_α^δ solving the optimization problem (17) may possess a subsequence which converges to a exact solution x^\dagger as $\delta \rightarrow 0$. Due to the Fréchet differentiability of the autoconvolution operator F and convexity of the applying penalty functionals $\mathcal{R}(x)$, for the numerical experiment below, we implement as second step the *sequential discrepancy principle (SDP)* which was analyzed, for example, in [2].

Definition 5. For given $\tau > 1$, $\alpha_0 > 0$, $0 < q < 1$, a parameter α_{SDP} is chosen from the set $\Delta_q := \{\alpha_l : \alpha_l = q^l \alpha_0, l \in \mathbb{Z}\}$ according to the sequential discrepancy principle (SDP), if

$$\|F(x_{\alpha_{SDP}}^\delta) - y^\delta\|_Y \leq \tau \delta < \|F(x_{\alpha_{SDP}/q}^\delta) - y^\delta\|_Y \quad (20)$$

holds true.

We can directly apply Theorem 1 from [2] to our autoconvolution problem and conclude that, with some $\bar{\delta} > 0$, the regularization parameters $\alpha_{SDP} = \alpha_{SDP}(\delta, y^\delta)$ chosen according to SDP exist for $0 < \delta < \bar{\delta}$ and satisfy the limit conditions (19). Then the associated regularized solutions $x_{\alpha_{SDP}(\delta, y^\delta)}^\delta$ converge (at least in the sense of subsequences) to exact solutions x^\dagger as $\delta \rightarrow 0$ and moreover $\lim_{\delta \rightarrow 0} \mathcal{R}(x_{\alpha_{SDP}(\delta, y^\delta)}^\delta) = \mathcal{R}(x^\dagger)$ holds true.

In a third step we search for *heuristic choices* of the regularization parameter $\alpha > 0$ provided that the noise level $\delta > 0$ is not available or reliable. In our numerical case studies we focus only on the quasi-optimality criterion to find $\alpha_{qo} = \alpha_{qo}(y^\delta)$, see [4, 5, 24] and references therein.

Definition 6. For sufficiently large $\alpha_0 > 0$ and for some $0 < q < 1$, we call the parameter α_{qo} chosen from the set $\Delta_q := \{\alpha_l : \alpha_l = q^l \alpha_0, l \in \mathbb{N}\}$ according to

$$\alpha_{qo}(y^\delta) = \operatorname{argmin}_{\alpha_l \in \Delta_q} \|x_{\alpha_l}^\delta - x_{\alpha_{l+1}}^\delta\|_X \quad (21)$$

quasi-optimal regularization parameter.

4.2 An iteratively regularized Gauss-Newton method

As an alternative we can also consider the iteratively regularized Gauss-Newton method (IRGNM) and find the minimizers of the functional

$$J_{\alpha_n}^\delta(x) := \|F(x_n^\delta) + F'(x_n^\delta)(x - x_n^\delta) - y^\delta\|_Y^2 + \alpha_n \mathcal{R}(x) \rightarrow \min_{x \in \mathcal{D}(F) \subseteq X}, \quad (22)$$

with some initial guess $x_0^\delta \in X$ for a fixed noise level $\delta > 0$. Therein, $F'(x) : X \rightarrow Y$ is the Fréchet derivative of F at $x \in X$ and a sequence $(\alpha_n)_{n \in \mathbb{N}}$ of regularization parameters satisfies

$$1 \leq \frac{\alpha_n}{\alpha_{n+1}} \leq C \quad (23)$$

with some constant $C > 0$. The central advantage of (22) over (17) is that x_{n+1}^δ is defined as the solution of a (due to linearity of $F'(x_n^\delta)$) **convex** optimization problem, which can efficiently be tackled by algorithms such as Chambolle-Pock [13] or FISTA [7]. By use of norm square penalty $\mathcal{R}_1(x)$, (22) can be solved explicitly as

$$(F'(x_n^\delta)^* [F'(x_n^\delta)] + \alpha_n \mathbb{I}) x = F'(x_n^\delta)^* [F'(x_n^\delta)x_n^\delta + y^\delta - F(x_n^\delta)] + \alpha_n \bar{x}. \quad (24)$$

Since the gradient operator is also linear, we can solve the linear equation

$$(F'(x_n^\delta)^* [F'(x_n^\delta)] + \alpha_n \nabla^* \nabla) x = F'(x_n^\delta)^* [F'(x_n^\delta)x_n^\delta + y^\delta - F(x_n^\delta)] \quad (25)$$

for the use of gradient norm square penalty $\mathcal{R}_2(x)$.

As a computational drawback, however, a full sequence of minimization problems (or linear equations) has to be solved. A convergence analysis for the IRGNM as depicted in (22) can e.g. be found in [22, 32].

Note that a similar approach has been proposed in [29], where the least-squares residuum $\|F(x) - y^\delta\|_Y^2$ is minimized on a finite dimensional ansatz space $x \in \text{span}\{\mu_1, \dots, \mu_n\}$ (e.g. consisting of splines) by linearization and iterative updating. In contrast to (17) and (22), regularization is there obtained by restriction to a finite-dimensional space, but the computational procedure is besides this comparable to our update formula in (22).

Instead of choosing a regularization parameter α in Tikhonov regularization, here we have to select an appropriate stopping index $n \in \mathbb{N}_0$. This can in principle be done by the same rules as discussed in section 4.1. The running index $n \in \mathbb{N}_0$ can be selected

- in the best case as n_{opt} with

$$n_{opt}(\delta) = \operatorname{argmin}_{n \in \mathbb{N}_0} \|x_n^\delta - x^\dagger\|_X;$$

- according to a-posteriori sequential discrepancy principle for a given constant parameter $\tau > 1$ as n_{SDP} if

$$\|F(x_{n_{SDP}}^\delta) - y^\delta\|_Y \leq \tau \delta < \|F(x_{n_{SDP}-1}^\delta) - y^\delta\|_Y$$

holds true, see [25] and the references therein.

5 Numerical treatment

5.1 Discretization via the composite midpoint rule

To discretize the continuous problem, we consider two different approaches. The first option is to divide each direction of the unit square equidistantly in n partitions with the uniform length $h := 1/n$. In order to discretize the nonlinear convolution equation or deduce the discretized forward operator, it is reasonable to replace the function values $x(t_1, t_2)$ and $y(s_1, s_2)$ by countable values $x_{i,j}$ and $y_{k,l}$ with

$$x_{i,j} := x\left(\frac{1}{2}(i + (i - 1))h, \frac{1}{2}(j + (j - 1))h\right), \quad y_{k,l} = y(kh, lh)$$

for all $i, j = 1, \dots, n$ and $k, l = 1, \dots, n$, respectively.

5.1.1 Discretization of forward operator for the limited data case

The autoconvolution equation in the limited data case can then by means of the composite mid-point rule be approximated by the discrete equation

$$\sum_{j=1}^l \sum_{i=1}^k h^2 x_{k-i+1, l-j+1} x_{i,j} = y_{k,l}. \quad (26)$$

Since the function x takes value only for $0 \leq t_1 \leq s_1$ and $0 \leq t_2 \leq s_2$, only the indices $i \leq k$ and $j \leq l$ need to be taken into consideration in the discretized version accordingly. Transforming the values $x_{i,j}$ and $y_{k,l}$ into vectors $\underline{x} := (x_1, \dots, x_p, \dots, x_{n^2})^\top$ and $\underline{y} := (y_1, \dots, y_q, \dots, y_{n^2})^\top$, respectively, with $p := (i-1) \cdot n + j$ and $q := (k-1) \cdot n + l$ for all $p, q = 1, \dots, n^2$, we can rewrite the weakly nonlinear forward operator of autoconvolution as

$$F_1(\underline{x}) := h^2 M_1(\underline{x}) \underline{x}, \quad (27)$$

where $M_1(\underline{x}) \in \mathbb{R}^{n^2 \times n^2}$ is a lower triangle block matrix and has the structure

$$M_1(\underline{x}) := \begin{pmatrix} B_1 & 0 & \cdots & 0 \\ B_2 & B_1 & \cdots & 0 \\ \vdots & \ddots & \ddots & \vdots \\ B_n & B_{n-1} & \cdots & B_1 \end{pmatrix} \text{ with } B_m = \begin{pmatrix} x_{(m-1)n+1} & 0 & \cdots & 0 \\ x_{(m-1)n+2} & x_{(m-1)n+1} & \ddots & 0 \\ \vdots & \ddots & \ddots & \vdots \\ x_{mn} & x_{m-1} & \cdots & x_{(m-1)n+1} \end{pmatrix}$$

for $1 \leq m \leq n$. The first derivative of $F_1(\underline{x})$ can then be easily obtained as

$$F_1'(\underline{x}) = 2h^2 M_1(\underline{x}).$$

5.1.2 Discretization of forward operator for the full data case

In the full data case, the discrete forward operator of the autoconvolution equation can be derived in a similar way. On four subareas $[0, 1]^2$, $[0, 1] \times (1, 2)$, $(1, 2) \times [0, 1]$ and $(1, 2)^2$ we have the discrete equations as:

$$\begin{aligned} \sum_{j=1}^l \sum_{i=1}^k h^2 x_{k-i+1, l-j+1} x_{i,j} &= y_{k,l} & \text{for } 1 \leq k, l \leq n \\ \sum_{j=l-n}^{n-1} \sum_{i=1}^k h^2 x_{k-i+1, l-j} x_{i, j+1} &= y_{k,l} & \text{for } 1 \leq k \leq n \text{ and } n+1 \leq l \leq 2n-1 \\ \sum_{j=1}^l \sum_{i=k-n}^{n-1} h^2 x_{k-i, l-j+1} x_{i+1, j} &= y_{k,l} & \text{for } n+1 \leq k \leq 2n-1 \text{ and } 1 \leq l \leq n \\ \sum_{j=l-n}^{n-1} \sum_{i=k-n}^{n-1} h^2 x_{k-i, l-j} x_{i+1, j+1} &= y_{k,l} & \text{for } n+1 \leq k, l \leq 2n-1. \end{aligned} \quad (28)$$

On the outside boundary of $[0, 2] \times [0, 2]$, i.e. for either $k = 2n$ or $l = 2n$, y vanishes. Note that the grid width remains $h = 1/n$. The discretized forward operator can be written as

$$F_2(\underline{x}) := h^2 M_2(\underline{x}) \underline{x}$$

with an extended block matrix $M_2(\underline{x}) \in \mathbb{R}^{4n^2 \times n^2}$, where

$$M_2(\underline{x}) := \begin{pmatrix} B_1 & 0 & \cdots & \cdots & 0 \\ C_1 & 0 & \cdots & \cdots & 0 \\ B_2 & B_1 & \cdots & \cdots & 0 \\ C_2 & C_1 & \cdots & \cdots & 0 \\ \vdots & \ddots & \ddots & \ddots & \vdots \\ B_n & B_{n-1} & \cdots & \cdots & B_1 \\ C_n & C_{n-1} & \cdots & \cdots & C_1 \\ 0 & B_n & B_{n-1} & \cdots & B_2 \\ 0 & C_n & C_{n-1} & \cdots & C_2 \\ \vdots & \ddots & \ddots & \ddots & \vdots \\ 0 & 0 & 0 & \cdots & B_n \\ 0 & 0 & 0 & \cdots & C_n \\ 0 & 0 & 0 & \cdots & 0 \\ 0 & 0 & 0 & \cdots & 0 \end{pmatrix} \quad \text{with } C_m = \begin{pmatrix} 0 & x_{mn} & x_{mn-1} & \cdots & x_{(m-1)n+2} \\ 0 & 0 & x_{mn} & \ddots & x_{(m-1)n+3} \\ \vdots & \ddots & \ddots & \ddots & \vdots \\ 0 & 0 & 0 & \cdots & x_{mn} \\ 0 & 0 & 0 & \cdots & 0 \end{pmatrix} \quad \text{and } B_m$$

as stated above for $1 \leq m \leq n$.

The first derivative of the extended forward operator is then given as $F'_2(\underline{x}) = 2h^2 M_2(\underline{x})$.

5.1.3 Discretization of the penalty functionals

The penalty functionals \mathcal{R}_1 and \mathcal{R}_2 can be discretized straight-forward, while the derivatives of ∇x are approximated by using finite differences. However, in order to ensure differentiability of the discretization of \mathcal{R}_3 , we take the approximation $\sqrt{|w_1|^2 + |w_2|^2 + \beta}$ for the 1-norm $\|w\|_1 = |w_1| + |w_2|$ of a vector $w = (w_1, w_2)$ with a small positive parameter $\beta \in (0, 1)$. This idea leads to the discretization

$$\begin{aligned} \mathcal{R}_3(x) \approx h & \left(\sum_{i=1}^{n-1} \sum_{j=1}^{n-1} \sqrt{(x_{i+1,j} - x_{i,j})^2 + (x_{i,j+1} - x_{i,j})^2 + h^2 \beta^2} \right. \\ & \left. + \sum_{i=1}^{n-1} \sqrt{(x_{i+1,n} - x_{i,n})^2 + h^2 \beta^2} + \sum_{j=1}^{n-1} \sqrt{(x_{n,j+1} - x_{n,j})^2 + h^2 \beta^2} \right), \end{aligned} \quad (29)$$

5.2 Discretization of forward operator via the Fourier transform

If we assume that the function $x \in L^2((0, 1)^2)$ can be extended on the whole domain \mathbb{R}^2 with the support of x $\text{supp}(x) \subset [0, 1] \times [0, 1]$, i.e. $x(t) = 0$ for $t = (t_1, t_2) \notin [0, 1]^2$, then we have the Fourier transform of x as

$$\mathcal{F}(x)(\omega) := \frac{1}{\sqrt{2\pi}} \int_{[0,1]^2} x(t) e^{i\omega t} dt, \quad \omega \in \mathbb{R}^2. \quad (30)$$

According to the convolution theorem, the autoconvolution operator can be represented by

$$F(x) = \mathcal{F}^{-1}(\mathcal{F}(x)^2) \quad (31)$$

Since the Fourier transform operator \mathcal{F} w.r.t. x is linear, we can easily obtain the Fréchet derivative and its adjoint operator of autoconvolution forward operator

$$\begin{aligned} F'(x)(u) &= \mathcal{F}^{-1}(2\mathcal{F}(x)\mathcal{F}(u)) \\ F'(x)^*(v) &= \mathcal{F}^{-1}(2\overline{\mathcal{F}(x)}\mathcal{F}(v)) \end{aligned} \quad (32)$$

for $u \in X$, $v \in Y$ and $\bar{\cdot}$ denotes the conjugated complex value.

A discretization of the above formulas is directly available by means of the Fast Fourier Transform (FFT) and its inverse (IFFT). However, we should take into account that they consider *periodic* functions, and hence the corresponding discretization will be erroneous especially close to the boundary and is not able to distinguish between the limited and the full data case.

For the limited data case we perform a zero-padding, i.e. replace the discretization $\underline{x} \in \mathbb{R}^{n \times n}$ by an extended matrix $\underline{x}^z \in \mathbb{R}^{2n \times 2n}$ of the form

$$\underline{x}^z = \begin{pmatrix} \underline{x} & 0 \\ 0 & 0 \end{pmatrix}.$$

More precisely, if we denote the zero-padding operator by $Z : \mathbb{R}^{n \times n} \rightarrow \mathbb{R}^{2n \times 2n}$ and the corresponding left-inverse (restriction) by $R : \mathbb{R}^{2n \times 2n} \rightarrow \mathbb{R}^{n \times n}$, then we obtain the discretization of (31) as

$$F(x) \approx R(\text{IFFT}(\text{FFT}(Z(\underline{x})))^2). \quad (33)$$

and the corresponding discretizations of (32) as

$$\begin{aligned} F'(x)(u) &\approx R(\text{IFFT}(2\text{FFT}(Z(\underline{x}))\text{FFT}(Z(\underline{u})))) \\ F'(x)^*(v) &\approx R(\text{IFFT}(2\overline{\text{FFT}(Z(\underline{x}))}\text{FFT}(Z(\underline{v})))) \end{aligned} \quad (34)$$

The only difference between the limited data and the full data case is whether the restriction R as to be applied as a very last step or not.

5.3 Computational implementation

In order to tackle the autoconvolution problem in a stable way, we can either solve the Tikhonov regularized problem (17) with diverse penalty functionals or solve the iteratively regularized problem (22) equipped with norm square penalty $\mathcal{R}_1(x)$ or gradient norm square penalty $\mathcal{R}_2(x)$. For both approaches, we need to initialize the regularization parameter α_0 and set the iteration step $q \in (0, 1)$ with $\alpha_l = q^l \alpha_0$ for $l = 1, 2, 3, \dots$.

To solve the Tikhonov regularized problem (17) with $\alpha := \alpha_l$, we use the discretization via the composite midpoint rule and consider its first-order optimality condition

$$2h^2(M(\underline{x}))^\top (h^2 M(\underline{x})\underline{x} - y^\delta) + \alpha \mathcal{R}'(\underline{x}) = 0, \quad (35)$$

which will be solved by using a damped Newton method. In this nonlinear equation, either $M := M_1$ is in use for the limited data case or $M := M_2$ for y^δ in the full data case. Note that the Newton-type method for solving (35) is also more or less a iterative procedure and needs initialization of solution as well.

For our academical experiments (x^\dagger is known), we carry out the process according to the following conceptual algorithm:

Algorithm 1 Conceptual algorithm for solving (17)

S0: Let $\{\delta_k\}_{k \in \mathbb{N}}$ be a finite sequence of positive noise levels tending to 0 as $k \rightarrow \infty$. Fix $\alpha_0 > 0$ and $0 < q < 1$. Set x_0 be a starting point, $l := 0$, $k := 0$ and $x_{\alpha_l}^{\delta_k} := x_0$.

S1: Compute the error $E_l^k = \|x_{\alpha_l}^{\delta_k} - x^\dagger\|_X$.

S2: Solve the discretized problem (35) for fixed $\delta := \delta_k$ and $\alpha := \alpha_l$ using a damped Newton method with starting point $x_{\alpha_l}^{\delta_k}$. Let $x_{\alpha_{l+1}}^{\delta_k}$ be the associated solution and compute the error

$$E_{l+1}^k = \|x_{\alpha_{l+1}}^{\delta_k} - x^\dagger\|_X.$$

S3: If $E_{l+1}^k < E_l^k$, then $\alpha_{l+1} := q\alpha_l$, $l := l + 1$ and go to **S2**. Otherwise save $x_{\alpha_l}^{\delta_k}$ and go to **S4**.

S4: Set $x_{\alpha_0}^{\delta_{k+1}} := x_{\alpha_l}^{\delta_k}$, $l := 0$, $k := k + 1$ and go to **S2**.

Note that this algorithm can be efficiently implemented due to the square rate of convergence of Newton-type method. However, the derivation of the first and second derivative of the autoconvolution operator and penalty functionals costs us a certain effort.

To solve the iteratively regularized problem (22) with either $\mathcal{R} := \mathcal{R}_1$ or $\mathcal{R} := \mathcal{R}_2$, more precisely, to solve the linear equations (24) and (25), we make use of Fourier transform technique to discretize

the forward operator and apply the CG (conjugate gradient) method. Besides benefiting the fast computation time, we can also save the trouble of derivation of second derivative matrices of all functionals. Actually, the associated algorithm is similar to Algorithm 1. The notation $x_{\alpha_l}^{\delta_k}$ in Algorithm 1 corresponds to the solution of (24) and (25) on the step $n := l$ for $\delta := \delta_k$.

6 Numerical experiments

In this section, we present case studies of numerical experiments based on both examples that had been introduced in Subsection 3.1. For all three penalties $\mathcal{R}_i(x)$ ($i = 1, 2, 3$) introduced above, properties and accuracy of regularized solutions are compared and illustrated for various regularization parameter choice rules. We define a sequence of finite discrete noise levels $\{\delta_k\}_{k \in \mathbb{N}}$ with corresponding relative noise levels between 10% and 0.05%. Let input data $y^{\delta_k} \in Y$ satisfy $\|y^{\delta_k} - y\|_Y = \delta_k$. In order to find appropriate regularization parameters α for each fixed δ_k , we set for the sequence $(\alpha_l)_{l \in \mathbb{N}}$ the starting value $\alpha_0 = 1$, step size $q = 0.5$ and thus $\alpha_{l+1} = \alpha_l/2$, see Algorithm 1. On the discretized domain with discretization level $n = 20$, we solve the nonlinear equation (35), discretized counterparts of linear equations (24) and (25) for each δ_k and the regularization parameter α_l . Additionally, the constant function $x_0 \equiv 1$ is set as initialization for all computations. For the use of penalty term $\mathcal{R}_1(x)$, the reference element is set as a constant function $\bar{x} = 0.5$. If we set $\bar{x} = -0.5$, the solutions $x_{\alpha_l}^{\delta_k}$ will converge to $-x^\dagger$ for both examples. Following the SDP choosing rule to determine the regularization parameters α_{SDP}^δ in Tikhonov regularized problem or the running index n_{SDP} in iteratively regularized problem, the constant parameter $\tau = 1.2$ is fixed for our experiments. By use of smoothed total variation the smoothing parameter β is fixed as 0.1 in the discretized TV penalty (29).

6.1 Results for Example 1

First we compare in Figure 4 the relative output errors of the regularized solutions $x_{\alpha_{opt}}^{\delta_k}$ obtained by using diverse penalties and by distinguishing the full data case and the limited data case. Since, for all penalties, the accuracies obtained with the full input data are uniformly better than those obtained with limited input data, we have illustrated in the following figure for the full data case only accuracies to the norm square penalty $\mathcal{R}_1(x)$ by use of Tikhonov regularization. On the other hand, results for all penalties and both regularization methods are displayed for the limited data case.

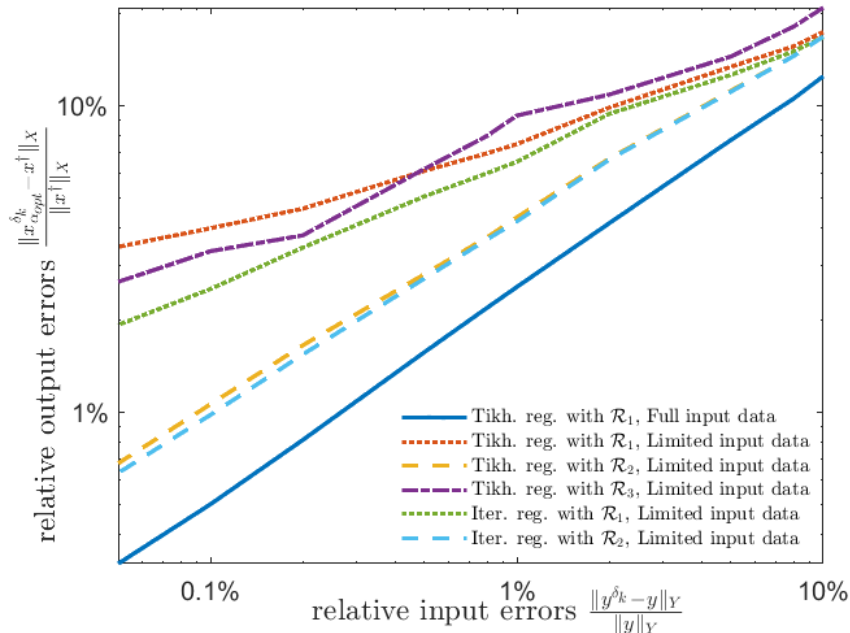


Figure 4: Comparison of relative error norms of regularized solutions $x_{\alpha_{opt}}^{\delta k}$ with optimal regularization parameter.

Obviously, the operation with the full input data brings the smallest and best output error. For the limited data case, the gradient norm square penalty is the most suitable for this example. A perspicuous reason is the high level of smoothness of the exact solution x^\dagger . The quality of Tikhonov-regularized solutions based on the classical norm square penalty \mathcal{R}_1 and of the TV-penalty \mathcal{R}_3 is almost indiscernible. Moreover, when using this gradient penalty \mathcal{R}_2 , the quality of results for Tikhonov regularization and iterative regularization are nearly not indistinguishable.

In Table 1 we present Hölder exponents $\kappa \in (0, 1)$ estimated by regression from a series of δ -values, which emulate numerically convergence rates results for regularized solutions with best possible regularization parameter α_{opt} for each δ . Precisely, we have listed the exponents κ such that approximately $\|x_{\alpha_{opt}}^\delta - x^\dagger\|_X \sim \delta^\kappa$ as $\delta \rightarrow 0$.

Table 1: Estimated Hölder exponents $\kappa \in (0, 1)$ for Hölder convergence rates $\|x_{\alpha_{opt}}^\delta - x^\dagger\|_X \sim \delta^\kappa$ as $\delta \rightarrow 0$

data situation penalty variation	full data case $Y = L^2([0, 2]^2)$			limited data case $Y = L^2([0, 1]^2)$		
	$\mathcal{R}_1(x)$	$\mathcal{R}_2(x)$	$\mathcal{R}_3(x)$	$\mathcal{R}_1(x)$	$\mathcal{R}_2(x)$	$\mathcal{R}_3(x)$
Tikhonov reg.	0.6946	0.6638	0.4685	0.3118	0.6015	0.3919
Iterative reg.	0.7184	0.6936	—	0.4088	0.6183	—

For the limited data case, the gradient norm square penalty also delivers the largest Hölder rate exponent for the regularized solutions with best possible regularization parameter, which is consistent with the insights from Figure 4 above. Partially, the rate exponents for the iterative regularization method seems to be higher than in case of Tikhonov regularization.

Next, we compare in Table 2 the regularized solutions with respect to different regularization

parameter chosen rules, representatively for a fixed noise level δ of a relative input error $\frac{\|y^\delta - y\|_Y}{\|y\|_Y} = 1\%$:

Table 2: Comparison of relative error norms of regularized solutions for a fixed relative input error 1%

relative input errors	Tikhonov reg.			Iterative reg.		
	$Y = L^2([0, 2]^2)$ $\mathcal{R}_1(x)$	$\mathcal{R}_1(x)$	$\mathcal{R}_2(x)$	$Y = L^2([0, 1]^2)$ $\mathcal{R}_3(x)$	$\mathcal{R}_1(x)$	$\mathcal{R}_2(x)$
$\frac{\ x_{\alpha_{opt}}^\delta - x^\dagger\ _X}{\ x^\dagger\ _X}$	2.56%	7.49%	4.32%	9.28%	6.56%	4.19%
$\frac{\ x_{\alpha_{SDP}}^\delta - x^\dagger\ _X}{\ x^\dagger\ _X}$	2.71%	9.12%	9.91%	13.77%	9.07%	9.88%
$\frac{\ x_{\alpha_{qo}}^\delta - x^\dagger\ _X}{\ x^\dagger\ _X}$	2.71%	9.12%	4.39%	10.30%	-	-

The regularized solutions with the regularization parameters via discrepancy principle can be obtained in a more stable way than the use of quasi-optimality criterion, especially in pursuance of iteratively regularized Gauss-Newton-Method.

For a more intuitive comparison of regularized solutions with least-square solutions which had been presented in Figure 3, we now illustrate Tikhonov regularized solutions with best possible regularization parameter, obtained with classical norm square penalty $\mathcal{R}_1(x)$ for the same noise level of 0.8% in Figure 5 in the limited and in the full data case, respectively.

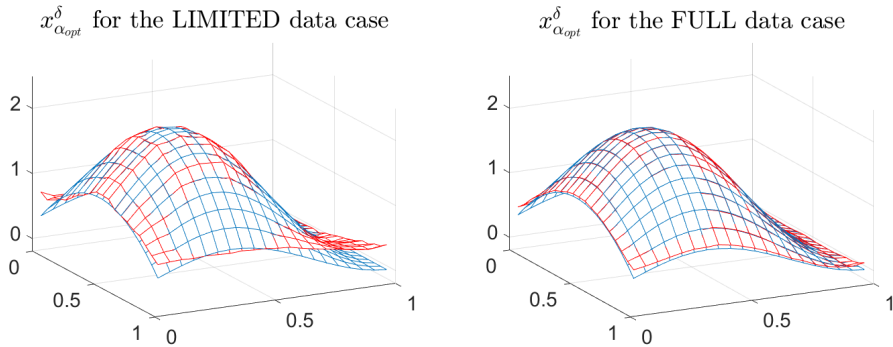


Figure 5: Regularized solutions with optimal regularization parameter for the limited and the full data case.

There are almost no longer oscillations in the images above. However, we can still observe the deviation of $x_{\alpha_{opt}}^\delta$ to the exact x^\dagger on the far back corner of the underlying unit square for the limited data case. These deviations can be eliminated by use of full input data.

6.2 Results for Example 2

Now we present analog results for Example 2 with x^\dagger from (15), which represents a non-smooth and non-factored function.

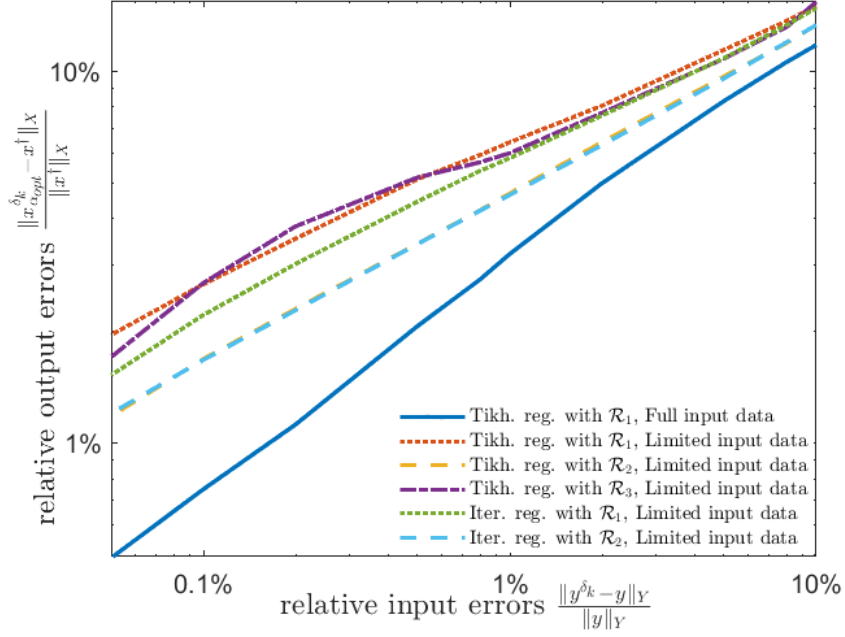


Figure 6: Comparison of relative error norms of regularized solutions $x_{\alpha_{opt}}^{\delta_k}$ with optimal regularization parameter.

The total variation penalty $\mathcal{R}_3(x)$ achieves progress among all penalties, since the function x^\dagger possesses jumps and is much less smooth compared to Example 1.

The Figure 7 shows the shapes of Tikhonov-regularized solutions with best possible regularization parameters, calculated for different penalties and limited input data by a relative noise level of 0.8%. The involvement of TV penalty $\mathcal{R}_3(x)$ can be especially observed on the rear area, where the function values tend to be constant. By contrast, the gradient norm square penalty $\mathcal{R}_2(x)$ makes the associated regularized solution more smooth on the front area.

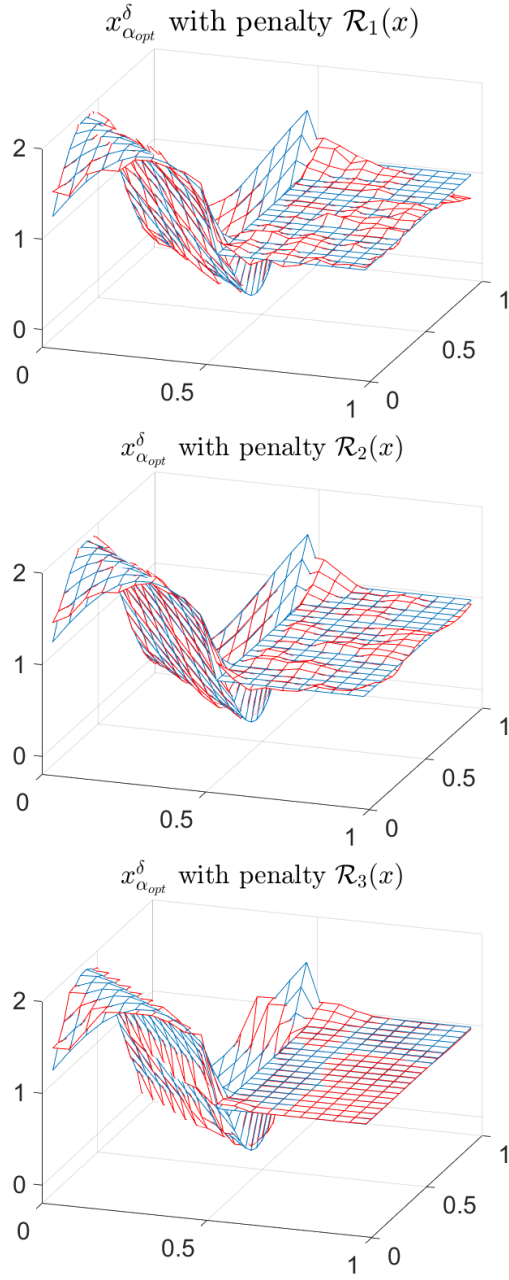


Figure 7: Regularized solutions obtained with optimal regularization parameter and for different penalties.

We again present also the estimated Hölder exponents κ for regularized solutions $x_{\alpha_{opt}}^{\delta_\kappa}$ with optimal regularization parameter.

Table 3: Estimated Hölder exponents $\kappa \in (0, 1)$ for Hölder convergence rates $\|x_{\alpha_{opt}}^\delta - x^\dagger\|_X \sim \delta^\kappa$ as $\delta \rightarrow 0$

data situation penalty variation	full data case $Y = L^2([0, 2]^2)$			limited data case $Y = L^2([0, 1]^2)$		
	$\mathcal{R}_1(x)$	$\mathcal{R}_2(x)$	$\mathcal{R}_3(x)$	$\mathcal{R}_1(x)$	$\mathcal{R}_2(x)$	$\mathcal{R}_3(x)$
Hölder exponent κ						
Tikhonov reg.	0.6059	0.6320	0.5083	0.3753	0.4522	0.3787
Iterative reg.	0.6699	0.6705	-	0.4164	0.4505	-

Regarding the convergence rates of $x_{\alpha_{opt}}^\delta$ converging to x^\dagger as $\delta \rightarrow 0$, for both penalties \mathcal{R}_1 and \mathcal{R}_2 the iterative regularization approach proves to be advantageous.

Similar to the Example 1, we list in Table 4 the relative output errors of regularized solutions $x_{\alpha_{opt}}^\delta$, $x_{\alpha_{SDP}}^\delta$ and $x_{\alpha_{qo}}^\delta$ for the fixed noise level δ of relative input error 1%.

Table 4: Comparison of relative error norms of regularized solutions for a fixed relative input error 1%

relative input errors	Tikhonov reg.			Iterative reg.		
	$Y = L^2([0, 2]^2)$ $\mathcal{R}_1(x)$	$\mathcal{R}_1(x)$	$\mathcal{R}_2(x)$	$Y = L^2([0, 1]^2)$ $\mathcal{R}_3(x)$	$\mathcal{R}_1(x)$	$\mathcal{R}_2(x)$
$\frac{\ x_{\alpha_{opt}}^\delta - x^\dagger\ _X}{\ x^\dagger\ _X}$	3.22%	6.43%	4.68%	6.01%	5.83%	4.64%
$\frac{\ x_{\alpha_{SDP}}^\delta - x^\dagger\ _X}{\ x^\dagger\ _X}$	5.75%	8.59%	7.75%	10.60%	9.06%	8.92%
$\frac{\ x_{\alpha_{qo}}^\delta - x^\dagger\ _X}{\ x^\dagger\ _X}$	3.47%	7.23%	5.83%	6.01%	-	-

By summarizing the case studies, we can state that it is always possible to solve the two-dimensional deautoconvolution problem in a rather stable way by either Tikhonov or iterative regularization. In this context, we also obtain a reasonably accuracy when the choice of the regularization parameter is appropriate.

Acknowledgment

Yu Deng and Bernd Hofmann are supported by the German Science Foundation (DFG) under the grant HO 1454/13-1 (Project No. 453804957).

References

- [1] R. Acar and C. R. Vogel, *Analysis of bounded variation penalty methods for ill-posed problems*, Inverse Problems, 10(6):1217-1229, 1994.
- [2] S. W. Anzengruber, B. Hofmann and P. Mathé, *Regularization properties of the sequential discrepancy principle for Tikhonov regularization in Banach spaces*, Appl. Anal., 93(7):1382-1400, 2014.
- [3] S. W. Anzengruber, S. Bürger, B. Hofmann and G. Steinmeyer, *Variational regularization of complex deautoconvolution and phase retrieval in ultrashort laser pulse characterization*, Inverse Problems, 32(3):035002 (27pp), 2016.

- [4] A. B. Bakushinskij, *Remarks on choosing a regularization parameter using the quasi-optimality and ratio criterion*, U.S.S.R. Comput. Maths. Math. Phys., 24:181–182, 1984.
- [5] F. Bauer and S. Kindermann, *The quasi-optimality criterion for classical inverse problems*, Inverse Problems, 24(3):035002, 2008.
- [6] J. Baumeister, *Deconvolution of appearance potential spectra*, In: Direct and inverse boundary value problems, Oberwolfach, 1989, Vol. 37 of *Methoden Verfahren Math. Phys.*, Peter Lang, Frankfurt am Main, pp. 1–13, 1991.
- [7] A. Beck and M. Teboulle, *A fast dual proximal gradient algorithm for convex minimization and applications*, Oper. Res. Lett. 42(1): 1–6, 2014.
- [8] S. Bürger and J. Flemming, *Deautoconvolution: a new decomposition approach vs. TIGRA and local regularization*, J. Inverse Ill-Posed Prob., 23(3):231–243, 2015.
- [9] S. Bürger, J. Flemming and B. Hofmann, *On complex-valued deautoconvolution of compactly supported functions with sparse Fourier representation*, Inverse Problems, 32(10):104006 (12pp.), 2016.
- [10] S. Bürger and B. Hofmann, *About a deficit in low order convergence rates on the example of autoconvolution*, Appl. Anal., 94(3):477–493, 2015.
- [11] S. Bürger and P. Mathé, *Discretized Lavrent’ev regularization for the autoconvolution equation*, Appl. Anal., 96(10):1618–1637, 2017.
- [12] M. Burger and S. Osher, *A guide to the TV zoo*, In: *Level set and PDE based reconstruction methods in imaging*, Lecture Notes in Math. Vol. 2090, Springer, pp. 1–70, Cham 2013.
- [13] A. Chambolle and T. Pock, *A first-order primal-dual algorithm for convex problems with applications to imaging*, J. Math. Imaging Vision, 40(1):120–145, 2011.
- [14] K. Choi and A. D. Lanterman, *An iterative deautoconvolution algorithm for nonnegative functions*, Inverse Problems, 21(3):981–995, 2005.
- [15] H.W. Engl, M. Hanke and A. Neubauer, *Regularization of Inverse Problems*, Kluwer, Dordrecht, 1996.
- [16] G. Fleischer, R. Gorenflo and B. Hofmann, *On the autoconvolution equation and total variation constraints*, ZAMM Z. Angew. Math. Mech., 79(3):149–159, 1999.
- [17] G. Fleischer and B. Hofmann, *On inversion rates for the autoconvolution equation*, Inverse Problems, 12(4):419–435, 1996.
- [18] J. Flemming, *Variational source conditions, quadratic inverse problems, sparsity promoting regularization. New results in modern theory of inverse problems and an application in laser optics*, Birkhäuser/Springer, Cham, 2018.
- [19] D. Gerth, B. Hofmann, S. Birkholz, S. Koke and G. Steinmeyer, *Regularization of an autoconvolution problem in ultrashort laser pulse characterization*, Inverse Problems in Science and Engineering, 22(2):245–266, 2014.
- [20] R. Gorenflo and B. Hofmann, *On autoconvolution and regularization*, Inverse Problems, 10(2):353–373, 1994.
- [21] B. Hofmann and O. Scherzer, *Local ill-posedness and source conditions of operator equations in Hilbert spaces*, Inverse Problems, 14(5):1189–1206, 1998.
- [22] T. Hohage and F. Werner, *Iteratively regularized Newton-type methods for general data misfit functionals and applications to Poisson data*, Numer. Math., 123(4):745–779, 2014.

- [23] J. Janno, *Laurent'ev regularization of ill-posed problems containing nonlinear near-to-monotone operators with application to autoconvolution equation*, Inverse Problems, 16(2):333–348, 2000.
- [24] S. Kindermann and A. Neubauer, *On the convergence of the quasioptimality criterion for (iterated) Tikhonov regularization*, Inverse Probl. Imaging, 2(2):291–299, 2008.
- [25] B. Kaltenbacher, A. Neubauer and O. Scherzer, *Iterative Regularization Methods for Nonlinear Ill-Posed Problems*, Radon Series on Computational and Applied Mathematics, Vol. 6, Walter de Gruyter, Berlin, 2008.
- [26] J. L. Lions, *Supports de produits de composition I* (in French), Comptes Rendus Acad. Sci. Paris, 232:1530–1532, 1951.
- [27] J. L. Lions, *Supports dans la transformation de Laplace* (in French), J. Analyse Math., 2:369–380, 1953.
- [28] O. Scherzer, M. Grasmair, H. Grossauer, M. Haltmeier and F. Lenzen, *Variational Methods in Imaging*, Series: Applied Mathematical Sciences, Vol. 167, Springer, New York, 2009.
- [29] K. Th. Schleicher, S. W. Schulz, R. Gmeiner and H.-U. Chun, *A computational method for the evaluation of highly resolved DOS functions from APS measurements*, Journal of Electron Spectroscopy and Related Phenomena, 31(1):33–56, 1983.
- [30] T. Schuster, B. Kaltenbacher, B. Hofmann and K. S. Kazimierski, *Regularization Methods in Banach Spaces*, Radon Series on Computational and Applied Mathematics, Vol. 10, Walter de Gruyter, Berlin/Boston, 2012.
- [31] E. C. Titchmarsh, *The zeros of certain integral functions*, Proc. London Math. Soc. (2), 25:283–302, 1926.
- [32] F. Werner, *On convergence rates for iteratively regularized Newton-type methods under a Lipschitz-type nonlinearity condition*, J. Inverse Ill-Posed Probl., 23(1):75–84, 2015.